


RESEARCH

Open Access



# Inhibition of ERK1/2 in cancer-associated pancreatic stellate cells suppresses cancer–stromal interaction and metastasis

Zilong Yan<sup>1</sup>, Kenoki Ohuchida<sup>1,2\*</sup> , Shuang Fei<sup>1</sup>, Biao Zheng<sup>1,3</sup>, Weiyu Guan<sup>1</sup>, Haimin Feng<sup>1</sup>, Shin Kibe<sup>1</sup>, Yohei Ando<sup>1</sup>, Kazuhiro Koikawa<sup>1</sup>, Toshiya Abe<sup>1</sup>, Chika Iwamoto<sup>2</sup>, Koji Shindo<sup>1</sup>, Taiki Moriyama<sup>1</sup>, Kohei Nakata<sup>1</sup>, Yoshihiro Miyasaka<sup>1</sup>, Takao Ohtsuka<sup>1</sup>, Kazuhiro Mizumoto<sup>4</sup>, Makoto Hashizume<sup>2</sup> and Masafumi Nakamura<sup>1\*</sup>

## Abstract

**Background:** Extracellular signal-regulated kinases (ERKs) have been related to multiple cancers, including breast cancer, hepatocellular cancer, lung cancer and colorectal cancer. ERK1/2 inhibitor can suppress growth of *KRAS*-mutant pancreatic tumors by targeting cancer cell. However, no studies have shown the expression of ERK1/2 on pancreatic stromal and its effect on pancreatic cancer–stromal interaction.

**Methods:** Immunohistochemistry and western blotting were performed to detect the expression of p-ERK1/2 in pancreatic tissues and cells. Cell viability assay was used to study IC<sub>50</sub> of ERK inhibitor on pancreatic cancer cells (PCCs) and primary cancer-associated pancreatic stellate cells (PSCs). Transwell migration, invasion, cell viability assay, senescence  $\beta$ -galactosidase staining were performed to determine the effect of ERK inhibitor on PCCs and PSCs in vitro and in vivo. The expression of key factors involved in autophagy and epithelial-to-mesenchymal transition (EMT) process were evaluated by western blotting. The expression of key factors related to cell invasiveness and malignancy were confirmed by qRT-PCR. Co-transplantation of PCC Organoid and PSC using a splenic xenograft mouse model was used to evaluate combined treatment of ERK inhibitor and autophagy inhibitor.

**Results:** Immunohistochemical staining in pancreatic tumor samples and transgenic mice detected p-ERK1/2 expression in both cancer cells and stromal cells. In pancreatic tissues, p-ERK1/2 was strongly expressed in cancer-associated PSCs compared with cancer cells and normal PSCs. PSCs were also significantly more sensitive to ERK1/2 inhibitor treatment. Inhibition of ERK1/2 suppressed EMT transition in HMPCCs, upregulated cellular senescence markers, activated autophagy in cancer-associated PSCs; and suppressed cancer–stromal interaction, which enhanced invasiveness and viability of cancer cells. We also found that chloroquine, an autophagy inhibitor, suppressed ERK inhibition-induced autophagy and promoted PSC cellular senescence, leading to significantly decreased cell proliferation. The combination of an ERK inhibitor and autophagy inhibitor suppressed liver metastasis in a splenic pancreatic cancer organoid xenograft mouse model.

**Conclusions:** These data indicate that inhibition of ERK1/2 in cancer-associated pancreatic stellate cells suppresses cancer–stromal interaction and metastasis.

**Keywords:** ERK1/2, Pancreatic cancer, Cancer–stromal interaction, Pancreatic stellate cell, Cellular senescence

\* Correspondence: [kenoki@surg1.med.kyushu-u.ac.jp](mailto:kenoki@surg1.med.kyushu-u.ac.jp);  
[mnaka@surg1.med.kyushu-u.ac.jp](mailto:mnaka@surg1.med.kyushu-u.ac.jp)

<sup>1</sup>Department of Surgery and Oncology, Graduate School of Medical Sciences, Kyushu University, 3-1-1 Maidashi, Fukuoka 812-8582, Japan  
Full list of author information is available at the end of the article



## Introduction

Pancreatic ductal adenocarcinoma (PDAC) is the fourth most common cause of cancer death worldwide, with a 5-year overall survival (OS) rate of only 5% [1]. The overwhelming majority of pancreatic cancer patients are diagnosed with liver metastasis [2], which is the leading primary cause of PDAC death, with a 5-year OS rate of 2.7% [3], and a median OS of less than 6 months [2]. As curative resection is not feasible after PDAC metastasizes to the liver [4], novel therapeutic strategies and agents are urgently needed in this setting.

Pancreatic cancer is characterized by excessive desmoplasia, which exhibited abundant tumor stromal in histology [5]. Tumor–stromal interactions reportedly promote PDAC progression and resistance to chemotherapies [6]. Pancreatic stellate cells (PSCs) are the primary stromal contributors to fibrosis in pancreatic disease [7]. PSCs transform from quiescent cells to activated myofibroblast-like cells through various stimuli, including interactions with tumor cells. Activated PSCs secrete cytokines that promote tumor cell proliferation and invasion [8]. As highly fibrotic stromal cells are seen in PDAC tumors and metastases, targeting stromal cells could be a therapeutic approach to PDAC [9].

Mitogen-activated protein kinases (MAPKs), also known as extracellular signal-regulated kinases (ERKs), act as an integration point for multiple biochemical signals, and affect such cellular processes such as proliferation, differentiation, transcription and development [10]. Two linked members of the MAPK family, ERK1 and ERK2, have been related to multiple human cancers, including breast cancer [11, 12], hepatocellular cancer [13], lung cancer [14] and colorectal cancer [15]. Two recent articles highlighted the functional role of p-ERK1/2 in pancreatic cancer and the therapeutic potential of inhibiting ERK1/2 activation. Principe et al. found p-ERK1/2 is necessary for TGF $\beta$ -induced epithelial–mesenchymal transition (EMT) in pancreatic cancer cells (PCCs), and found inhibition of p-ERK1/2 to both reduce CDK2 levels and prevent EMT [16]. Hayes et al. used ERK1/2 inhibitor on *KRAS*-mutant PDAC cells, and discovered an association between p-ERK1/2 and downstream c-MYC, with effects on cancer cell growth suppression and cellular senescence [17]. To date, however, no studies have shown the effects of ERK1/2 inhibitors on PSCs derived from pancreatic cancer tissues.

In the present study, we provide the first investigation of p-ERK1/2 expression on PSCs, and evaluate the sensitivity of PSCs to ERK1/2 inhibitor. We assessed the effects of ERK1/2 inhibitors on human PDAC cancer–stromal interaction. We also found that combining ERK1/2 inhibitor with chloroquine (CQ), an autophagy inhibitor, remarkably suppressed cancer–stromal interaction on cancer progression, both in vitro and in vivo. Taken together, our findings suggest that ERK1/2 promotes

pancreatic cancer–stromal interaction and metastasis, and is a promising target for treatment of PDAC.

## Materials and methods

### Pancreatic tissues

We obtained PDAC specimens from patients who underwent pancreatectomy for at our institution. KPC (LSL-Kras G12D/+; LSL-Trp53R172H/+; Pdx-1-Cre) transgenic mice were described previous [18]. Tissues were embedded, sliced, stained and observed using an optical microscope (BZ-X710; Keyence, Osaka, Japan).

### Immunohistochemistry

We blocked endogenous peroxidase activity with methanol containing 0.3% hydrogen peroxidase. Antigen retrieval was performed by boiling samples in a microwave oven (citrate buffer, pH 6.0). Human pancreatic tissues and KPC mice tissues were sliced to 4  $\mu$ m, incubated with rabbit anti-phospho-ERK1/2 (#4370, Cell Signaling, Technology, Danvers, MA, USA) overnight at 4 °C and stained with EnVision $\beta$  System-HRP Labeled Polymer Anti-Rabbit (#K4003; Dako, Glostrup, Denmark). The staining was performed using serial sections.

### Cells and culture conditions, and treatment

We used the following PCC lines: AsPC-1, CFPAC-1 (American Type Culture Collection, Manassas, VA, USA), Panc-1 (Riken BioResource Center, Ibaraki, Japan), SUIT-2 (Japan Health Science Research Resources Bank, Osaka, Japan), and BxPC-3 (National Kyushu Cancer Center, Fukuoka, Japan). All PCCs were maintained in DMEM (Sigma Chemical Co., St. Louis, MO, USA) supplemented with 10% FBS at 37 °C with humidified 90% air and 10% CO<sub>2</sub>. Human pancreatic ductal epithelial (HPDE) cells were obtained from Dr. M.-S. Tsao (University of Toronto, Canada) and maintained in HuMedia-KG2 medium (KK-2150S Kurabo, Osaka, Japan). We established human PSCs from fresh pancreatic cancer surgical specimens using the outgrowth method [19–21], as described in our previous reports. The isolated cells were confirmed to be PSCs by their spindle-shaped morphology, and immunofluorescence staining for  $\alpha$ SMA, vimentin, CD90, glial fibrillary acidic protein, and nestin, but not CK19 [22, 23]. They were used within eight passages for each assay. Immortalization of PSCs was conducted as described previous [23]. All PSCs were maintained in DMEM (Sigma-Aldrich Co., Tokyo, Japan) supplemented with 10% fetal bovine serum, streptomycin (100 mg/ml), and penicillin (100 mg/ml) at 37 °C in a humidified atmosphere containing 10% CO<sub>2</sub>. HPaSteC cells (#3830; ScienCell Research Laboratories, Carlsbad, CA, USA) were maintained according to the manufacturer's instructions using Stellate Cell Medium (#5301; ScienCell). PCCs

from primary tumors in KPC mice were established using an outgrowth method [19], and isolated cancer cell lines were maintained as described [24]. ERK1/2 inhibitor used in vitro (S7101, Selleck Chemicals, Houston, TX, USA) and in vivo (HY-50846, MCE, NJ, USA) were reconstituted following the manufacturer's recommendations and used at the indicated doses. Chloroquine phosphate was purchased from Sigma-Aldrich (#PHR1258), dissolved in phosphate-buffered saline to 10 mM, and stored at  $-20^{\circ}\text{C}$  until used.

#### PDAC organoid culture

PDAC organoids were established from KPC PCCs, which were established using the outgrowth method as described [21]. PCCs were embedded in growth factor-reduced Matrigel (Cat#356231; BD Bioscience, CA, USA), and cultured in human complete medium at  $37^{\circ}\text{C}$  for 14 days [21, 25]. Human complete medium was AdDMEM/F12 (Cat#12634-010; Invitrogen, CA, USA), medium supplemented with 1 M HEPES (Invitrogen), GlutaMax (Cat#35050-061; Invitrogen), penicillin/streptomycin (Cat#15140122; Invitrogen), B27 (Cat#17504044; Invitrogen), N-acetyl-L-cysteine (Cat#A9165; Sigma-Aldrich Co.), Wnt-3a (Cat#5036-WN-010; R&D Systems, MN, USA), R-Spondin 1 (Cat#120-38; Peprotech, NJ, USA), Noggin (Cat#120-10C; Invitrogen), epidermal growth factor (EGF, Cat#AF-100-15; Peprotech), fibroblast growth factor (FGF, Cat#100-26; Peprotech), nicotinamide (Cat#N0636; Sigma-Aldrich Co.), Y-27263 (Cat# Y0503; Sigma-Aldrich Co.) and A83-01 (Cat#2939/10; R&D Systems).

#### Quantitative reverse transcriptional-polymerase chain reaction (qRT-PCR)

Total RNA was extracted from cultured cells using a High Pure RNA Isolation Kit (Roche Diagnostics, Mannheim, Germany) and DNase I (Roche Diagnostics, Sigma-Aldrich), according to the manufacturers' instructions. We performed qRT-PCR using a QuantiTect SYBR Green Reverse Transcription-PCR kit (Qiagen, Tokyo, Japan) and a CFX96 Touch Real-Time PCR Detection System (Bio-Rad Laboratories, Hercules, CA). Our specific primer sequences were purchased from Sigma-Aldrich (Tokyo, Japan). Primer sequences are listed in Additional file 5: Table S1. We normalized mRNA expression levels to 18S rRNA levels.

#### Matrigel invasion and migration assay

The invasiveness and migration capacities of PCCs were assessed by determining the number of cells invading or migrating across transwell chambers as previously described [24, 26]. For invasion assays, PCCs ( $1 \times 10^5$  cells/250  $\mu\text{l}$ ) were seeded in the upper transwell chamber (8- $\mu\text{m}$  pore size; Becton Dickinson, Franklin Lakes, NJ) containing 100 mL of reconstituted Matrigel-coated

membrane (20 mg/well, BD Biosciences, Bedford, MA). Thereafter, cells were incubated for 36–48 h and the number of invading PCCs was counted. Cell migration assays were performed with PCCs using the same protocol as the invasion assay without a Matrigel-coated membrane. Cells were allowed to migrate, and were counted 18–24 h after cell seeding into the upper chamber. In co-culture experiments, PSCs were seeded in 24-well plates (#353504; Corning) at a density of  $5 \times 10^4$  cells/well. At 24 h after seeding, medium was replaced with 750  $\mu\text{L}$  of fresh DMEM containing 10% FBS. Transwell chambers (8- $\mu\text{m}$  pores; Becton Dickinson) were placed in 24-well dishes, and then PCCs, which had been suspended in 250  $\mu\text{L}$  of the same medium ( $1 \times 10^5$  cells/mL) were seeded into the transwell chambers. After incubation for the indicated time, migration and invasion were evaluated by counting the cells that had invaded to the lower chamber. In both assays and at each time point, invaded or migrated cells at the bottom of the chamber were fixed with 70% ethanol, stained with hematoxylin and eosin, and counted in 5 random fields at 100 $\times$  magnification (BZ-X710; Keyence Corporation, Osaka, Japan). Each experiment was performed in triplicate and repeated at least three times.

#### Western blot analysis

Western blotting was performed as described previously [27]. Cells were lysed in Pro-Prep (InTron Biotechnology, Seongnam, Korea) and proteins were separated on 4–15% Mini-Protean TGX Precast Gels (Bio-Rad) and transferred to Trans-Blot Turbo Mini PVDF Transfer Packs (Bio-Rad) using a Trans-Blot Turbo Transfer Starter System (Bio-Rad). Membranes were incubated overnight at  $4-8^{\circ}\text{C}$  with anti-ERK1/2 (#4695, Cell Signaling Technology, Danvers, MA, USA), anti-phospho-ERK1/2 (#4370, Cell Signaling Technology), anti- $\alpha\text{SMA}$  (#M0851; Dako, Japan), anti-E-cadherin (#3195S, Cell Signaling Technology), anti-vimentin (#5741, Cell Signaling Technology), anti-collagen type I (sc-8783 Santa Cruz Biotechnology, Santa Cruz, CA, USA), anti-collagen type VI (sc-47,712, Santa Cruz Biotechnology), anti-MMP2 (#13132, Cell Signaling Technology), anti-MMP3 (#sc-6839, Santa Cruz Biotechnology), anti-MMP14 (AB8345, Millipore, Temecula, CA, USA), anti-IL-6 (#ab9324, Abcam, Cambridge, MA, USA), anti-p16 (MABE1328, Millipore), anti-p15 (MABE1664, Millipore), anti-CC8 (#9496S, Cell Signaling Technology), anti-fibronectin (sc6952, Santa Cruz Biotechnology), anti-LC3 (#2775S; Cell Signaling Technology), anti-AKT (#4060S, Cell Signaling Technology), anti-phospho-AKT (#4691S, Cell Signaling Technology), and anti-b-actin (ab8227; Abcam), and then probed with appropriate secondary antibodies (Cell Signaling Technology). Immunoblot signals were detected by enhanced chemiluminescence with ChemiDoc XRS (Bio-Rad).

### Cell viability assay

Cells ( $1 \times 10^3$  cells/well) were seeded in 96-well plates (Greiner Bio-One, Frickenhausen, Germany) and cell viability examined using the CellTiter-Glo Luminescent Cell Viability Assay Kit (G7570, Promega) following the manufacturer's instructions. Background was subtracted using values from wells containing only culture medium.

### In vivo experiments

BALB/c A/Jcl *nu/nu* female mice were purchased from Clea (Tokyo, Japan) and transported to our institution at 4 weeks old. After 1 week of acclimation, each of the 20 nude mice were splenic implanted with  $5 \times 10^4$  PDAC organoids and  $5 \times 10^4$  PSCs and randomized into four groups for treatment with PBS (control), ERK1/2 inhibitor (25 mg/kg dissolved in 100  $\mu$ L PBS) alone, CQ (50 mg/kg dissolved in 100  $\mu$ L PBS) alone, or with a combination of ERK1/2 inhibitor and CQ. One week after implantation, mice were treated intraperitoneally with either vehicle, SCH772984, Chloroquine or combination according to the dosing schedule indicated in the figure legends. The mouse liver metastasis tissues were fixed in formaldehyde, embedded in paraffin, and cut into 4- $\mu$ m-thick sections. All mouse experiments were approved by the Ethics Committee of Kyushu University.

### Statistical analysis

For in vitro experiments, values are expressed as mean  $\pm$  standard deviation. Comparisons between two groups were made using Student's *t*-test.  $P < 0.05$  was considered significant.

## Results

### Establishment and characterization of highly metastatic PCCs

Three consecutive rounds of in vivo selection were performed by using splenic xenografts of PDAC cell lines SUI-2 and AsPC-1 cells, from which metastatic lesions were harvested to establish metastatic SUI-2 (SLMS) and AsPC-1 (SLMA) cells (Fig. 1a). We then investigated in vitro characteristics of the SLMS and SLMA cells. The SLMS cells had an apparent spindle-shaped morphology compared with their parental SUI-2 cells (Fig. 1b). Migration, invasion and proliferation capacities of highly metastatic (HM) PCCs were significantly greater than their parental PCCs (Fig. 1c, d; Additional file 1: Figure S1A). We confirmed that SLMS cells occurred in liver metastases more frequently than did their parental SUI-2 cells in vivo (Fig. 1e; Additional file 1: Figure S1B). As we had verified the upregulated aggressiveness of metastatic cells, we compared results of phospho-kinase array analysis between SLMS cells and parental SUI-2 cells, and found altered expression of several phosphorylation kinases HMPCCs,

including upregulation of p53 (S15), p53 (S46), AKT (S473), ERK1/2 (T202/Y204), AMPKa1 (T183), and downregulation of p70S6 kinase (T241/S424) and AMPKa2 (T172) (Additional file 1: Figure S1C). The greatest increase in phosphorylation level was seen in ERK1/2 (T202/Y204). To validate the accuracy of array data, we used western blotting to evaluate expression of p-ERK1/2 in HMPCCs and parental cells. We also found the mesenchymal marker vimentin was upregulated in HMPCCs (Additional file 1: Figure S1D). These data indicated that established HMPCCs were more aggressive and tumorigenic than their parent cells.

### Expression of p-ERK1/2 in pancreatic cancer tissues and cells

In previous reports, p-ERK1/2 expression in PCCs was demonstrated in pancreatic cancer tissues. Using database of Human Protein Atlas (available from www.proteinatlas.org), we found expression of ERK1 and/or ERK2 in both tumor and stromal cells (Additional file 2: Figure S2A, B). However, analysis of The Cancer Genome Atlas [28, 29] shows expression of ERK2, but not ERK1, correlates with poorer overall and disease-free survival in PDAC (Additional file 2: Figure S2C, D). We therefore investigated p-ERK1/2 expression in PDAC samples obtained in our institution (Additional file 6: Table S2) and detected p-ERK1/2 on both tumor cells and stromal cells (Fig. 2a). We also assessed p-ERK1/2 expression in PDAC derived from our KPC mouse model (LSL-KrasG12D/+; LSL-Trp53R172H/+; Pdx-1-Cre) and found p-ERK1/2 expression in primary tumor cells, stromal cells and liver metastases (Fig. 2b). Next, we investigated the p-ERK1/2 expression of various pancreatic cells including HPaStC cells (normal PSC cells), cancer-associated PSCs, HPDE cells and PCCs. PSCs showed high p-ERK1/2 expression, even compared with PCCs (Fig. 2c). Interaction between PCC and PSC is a key process in pancreatic cancer progression [30]. To validate the involvement of p-ERK1/2, we co-cultured PCCs and PSCs, using the transwell system. Compared with monocultured cells, p-ERK1/2 expression was significantly upregulated in PCCs when co-cultured with PSCs (Fig. 2d). Previous study showed that PSCs can promote migration, invasion and EMT process via the regulation of E-cadherin and vimentin expression in PDAC cells [31]. We also found that cell migration and invasion of AsPC-1 and SUI-2 were enhanced when indirectly co-cultured with PSCs (Fig. 2e and f).

### SCH772894 suppressed PCCs proliferation and epithelial-mesenchymal transition

Next, we investigated the effect of ERK inhibition on PCCs and PSCs. We chose a novel ERK1/2-selective pharmacologic inhibitor, SCH772984, which has shown

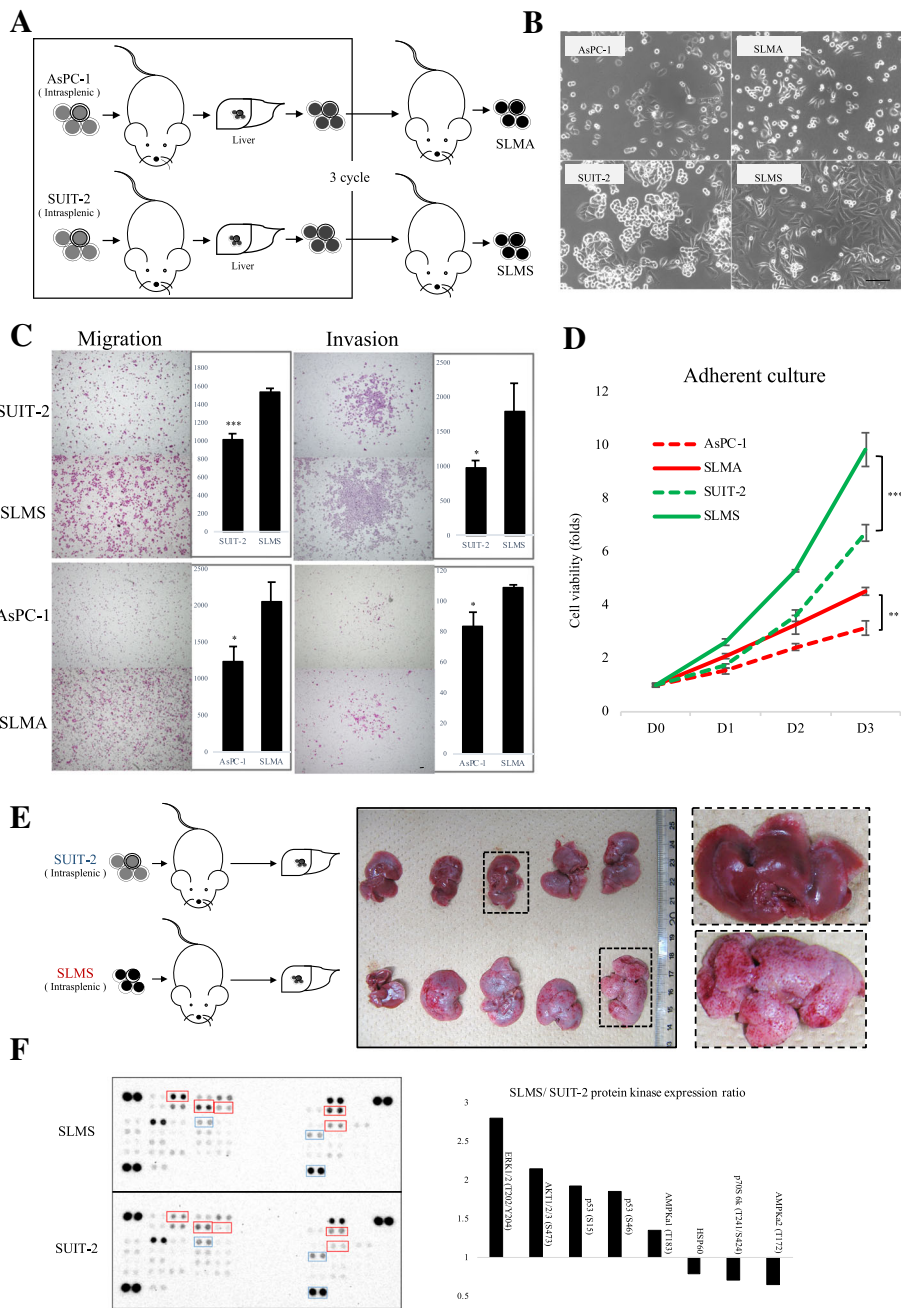


**Fig. 1** Establishment of highly metastatic PCCs. **a** Establishing PDAC cells. Parental PDAC cells were splenic transplanted into nude mice; liver metastases were harvested after 2–4 weeks. This process was performed 3 times. **b** Cellular morphology of parental PDAC cells and highly metastatic PDAC cells. Scale bars = 100 μm. **c** Migration and invasion assays were performed over 36 and 18 h respectively. Graphs show numbers of cells calculated from five fields. Original magnification: 40x. Scale bars = 100 μm. \*P < 0.05, \*\*\*P < 0.001. **d** Cell viability of cancer cells as determined by CellTiter-Glo luminescent cell viability assay. \*P < 0.05, \*\*P < 0.01. **e** SUI-2 and SLMS cells were intrasplenically injected in nude mice and the liver metastases were harvested. Gross pathology indicated metastatic lesions. **f** Phospho-protein kinase array of SUI-2 and SLMS cells. Right: most significant gene alterations

cellular potency in tumor cells with *BRAF*, *NRAS*, or *KRAS* mutations and induces tumor regressions in xenograft models at toxicity-free doses [32]. First, we examined the effects of SCH772984 on viability of parental PCCs and HMPCCs. The IC<sub>50</sub> values of

SCH772984 on AsPC-1 and SUI-2 cells were 1291 nM and 1180 nM, respectively (Fig. 3a, b), compared with 424.2 nM and 847.7 nM, respectively, for HM SLMA and SLMS cells, which indicates HMPCCs are more sensitive to ERK1/2 inhibitor (Fig. 3c, d). As

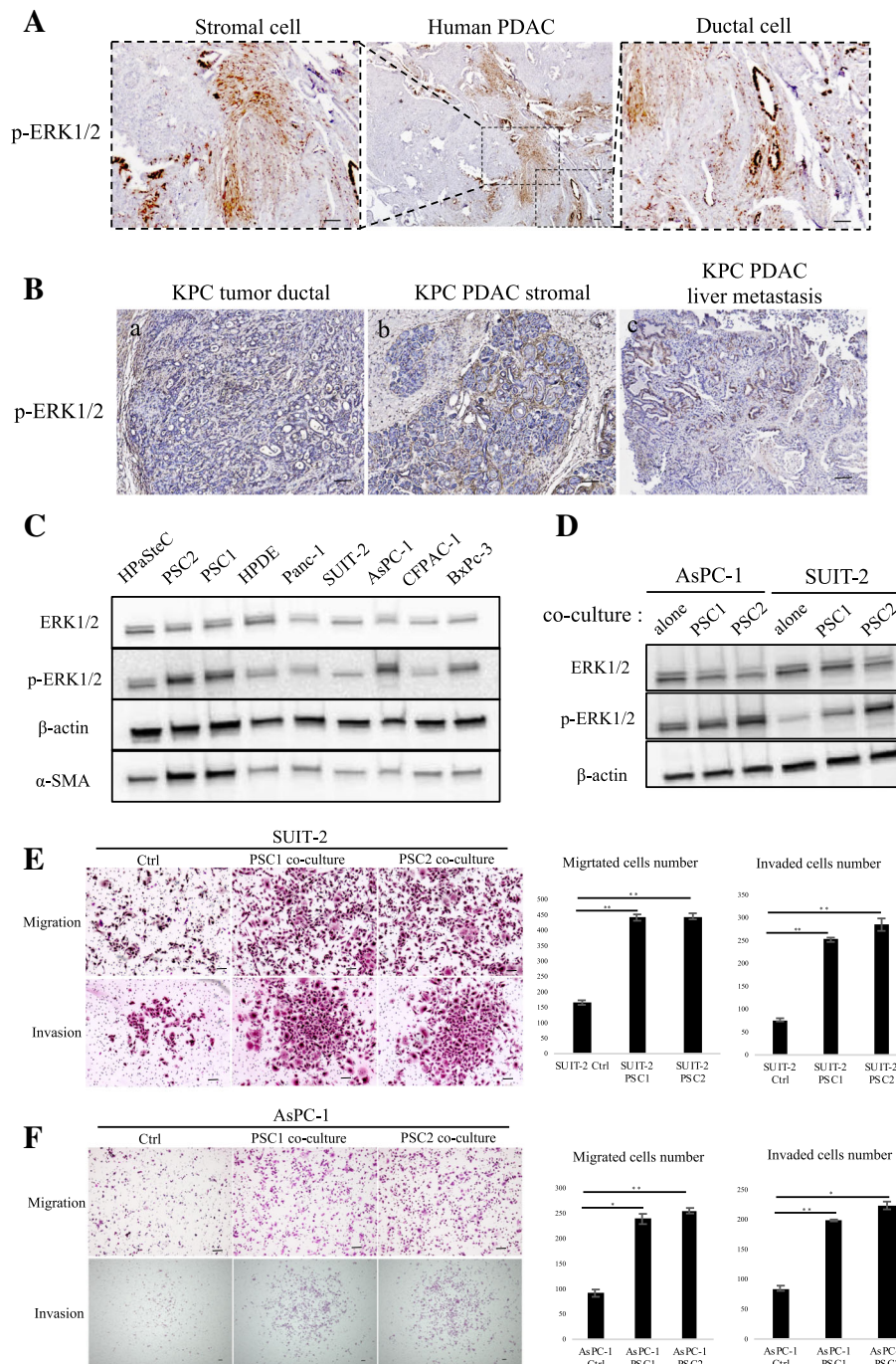


**Fig. 2** Expression of p-ERK1/2 in PDAC tissues and pancreatic cell lines. **a** p-ERK1/2 expression was detected in both pancreatic cancer cells and stromal cells. Scale bars =100  $\mu$ m. **b** p-ERK1/2 expression was detected in KPC mice cancer cells (**a**) and stromal cells (**b**) of pancreatic primary tumor, and liver metastases (**c**). Scale bars =100  $\mu$ m. **c** Western blot of ERK1/2, p-ERK1/2, and  $\alpha$ -SMA levels in pancreatic cells. **d** Western blot of ERK1/2 and p-ERK1/2 levels in PCCs, alone or after co-culture with PSCs. PCCs were seeded in 24-well plates while PSCs were seeded in the upper transwell chamber with 3- $\mu$ m pore size. **e** SUIIT-2, (**f**) AsPC-1 Migration and invasion assays were performed for 18 and 36 h, respectively. PSCs were seeded in 24-well plates while PCCs were seeded in the upper transwell chamber of 8- $\mu$ m pore size. Graphs show numbers of cells calculated from five fields. Scale bars =100  $\mu$ m. \* $P$  < 0.05, \*\* $P$  < 0.01

expression of p-ERK1/2 in PDAC is reportedly related to EMT [33], we investigated changes in kinase phosphorylation in HMPCCs after ERK1/2 inhibition.

Upregulation of the epithelial cell marker, E-cadherin, and downregulation of the mesenchymal marker, vimentin, were observed through western blotting

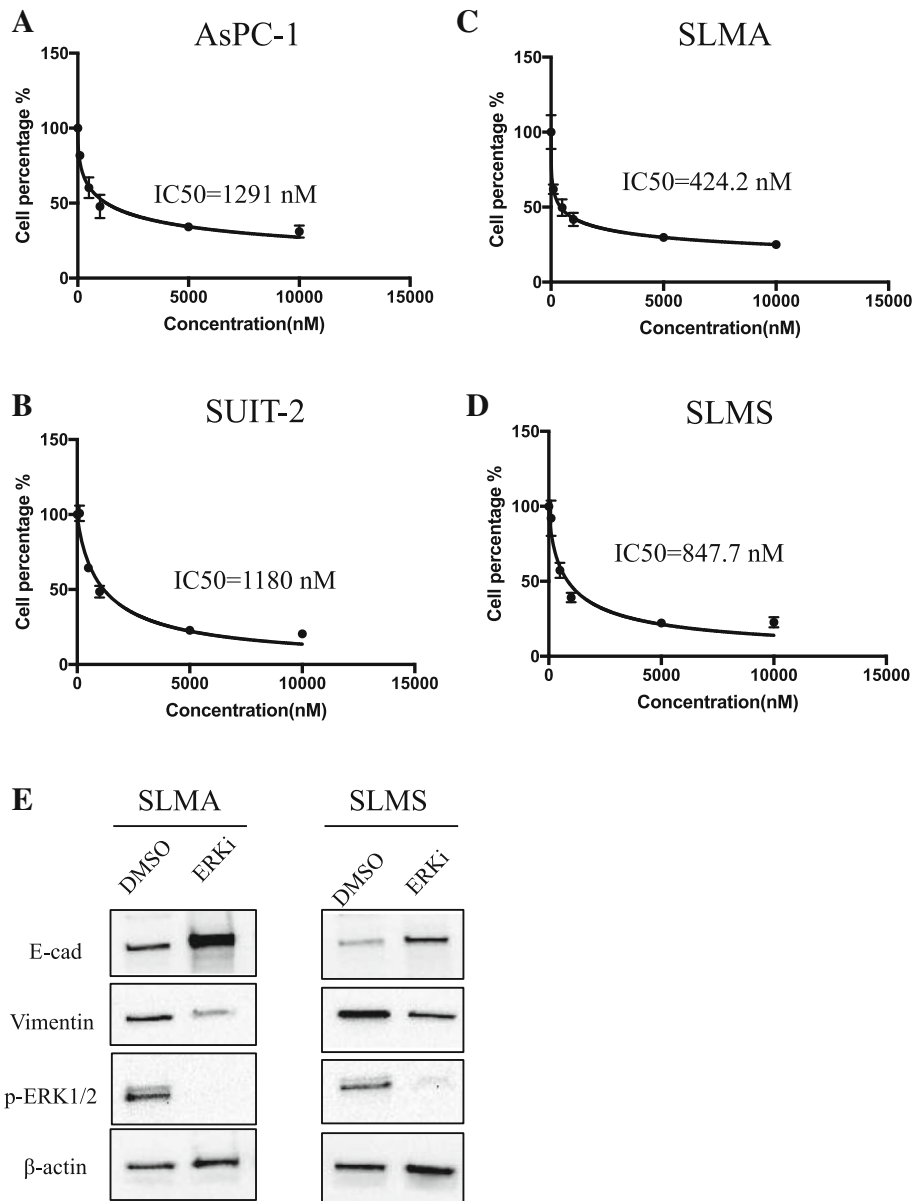


**Fig. 3** Inhibition of ERK1/2 decreased PDAC cell viability and EMT transition. **a** AsPC-1, **(b)** SUIT-2, **(c)** SLMA, and **(d)** SLMS cell viability after 72 h; treatment with various concentrations of ERK inhibitor after. IC<sub>50</sub> values are indicated. **e** Western blot of E-cadherin, vimentin, and p-ERK1/2 levels of highly metastatic cancer cells after treatment with ERK inhibitor SCH772984 at IC<sub>50</sub> value. The indicated protein was extracted exclusively from the living adherent cells. Negative control: DMSO

(Fig. 3e), which indicates that inhibiting p-ERK1/2 leads to suppression of EMT in HMPCCs.

**SCH772984 suppressed pancreatic stellate cell proliferation and induced upregulation of cellular senescence marker**

As high expression of p-ERK1/2 was only detected in PSCs (Fig. 2c), we hypothesized inhibiting ERK1/2 in PSCs would be more efficient than in PCCs. We established immortalized PSCs from a pancreatic cancer specimen obtained at our institution [34]. We observed a

change from spindle-like shapes to round shapes among these PSCs after 72 h of SCH772984 treatment (Fig. 4a). The two primary cultures of PSCs were more sensitive to SCH772984, with IC<sub>50</sub> values of 321 nM and 89 nM, respectively, compared with the HMPCCs (Fig. 4b, c). When we investigated changes in expressions of related cytokines and chemokines after SCH772984 treatment, we found senescence marker p15, p16, fibrosis marker α-SMA, fibronectin, Collagen Type I and Collagen Type IV were upregulated; and MMP2, MMP3, IL-6 (which are related to cell invasiveness and malignancy) were

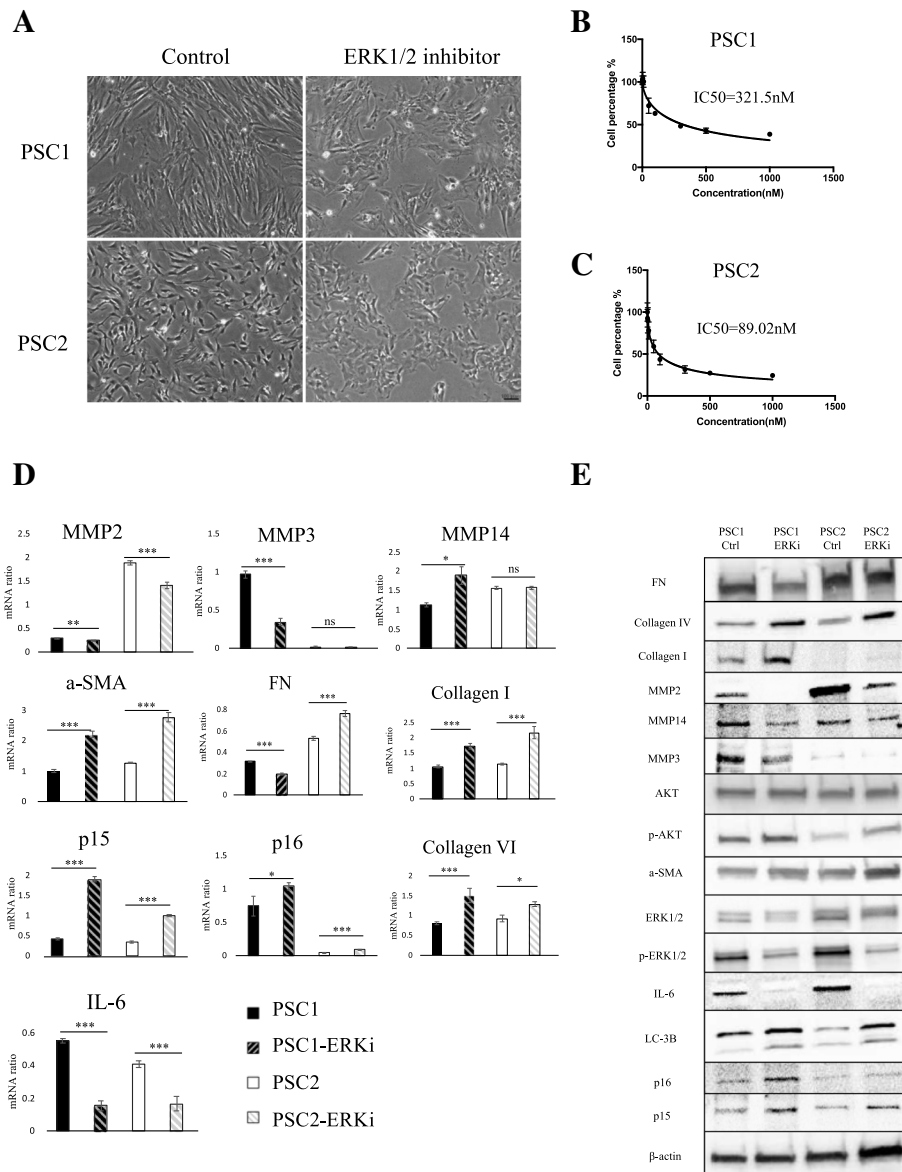


**Fig. 4** Inhibition of ERK1/2 facilitated PSCs atrophy and induces p16, α-SMA. **a** Microphotograph of PSCs after treatment with DMSO and/or ERK inhibitor. Scale bars = 100 μm. **b** Viability of PSC1 and **(c)** PSC2 cells, as determined by CellTiter-Glo luminescent cell viability assay after 72 h' treatment with indicated concentrations of ERK inhibitor; IC<sub>50</sub> values are indicated. **d** qRT-PCR of PSCs shows mRNA expression changes after ERK inhibitor treatment. \**P* < 0.05, \*\**P* < 0.01, \*\*\**P* < 0.001. **e** The indicated protein levels of PSCs were evaluated after treatment with DMSO as control and/or ERK inhibitor SCH772984 at IC<sub>50</sub> value

downregulated (Fig. 4d, e). These data are consistent with the results of the previous study, which showed that p16 induces cellular senescence and stable growth arrest without a senescence-associated secretory phenotype [35]. As inhibition of CDK4/6, a downstream target of ERK1/2, reportedly upregulated drug-induced autophagy in breast cancer [36], we investigated the effect of ERK inhibition on autophagy in PSCs. We found that autophagy marker LC-3II protein expression was upregulated. Our results suggest that inhibition of ERK did not induce the reversion of PSC from activated

phenotype to quiescent type, but to cellular senescence, which may be another activated phenotype.

**SCH772984 suppressed cancer–stromal interactions in PCCs that enhance migration, invasiveness and viability**

Because PCCs and PSCs showed similar reactions to SCH772984, we investigated the effect of SCH772984 on cancer–stromal interaction. Using a transwell indirect co-culture system (Fig. 5a), we found SCH772984 did not reduce PCC migration or invasion capacity when treated with the lower IC<sub>50</sub> dose for PSCs.



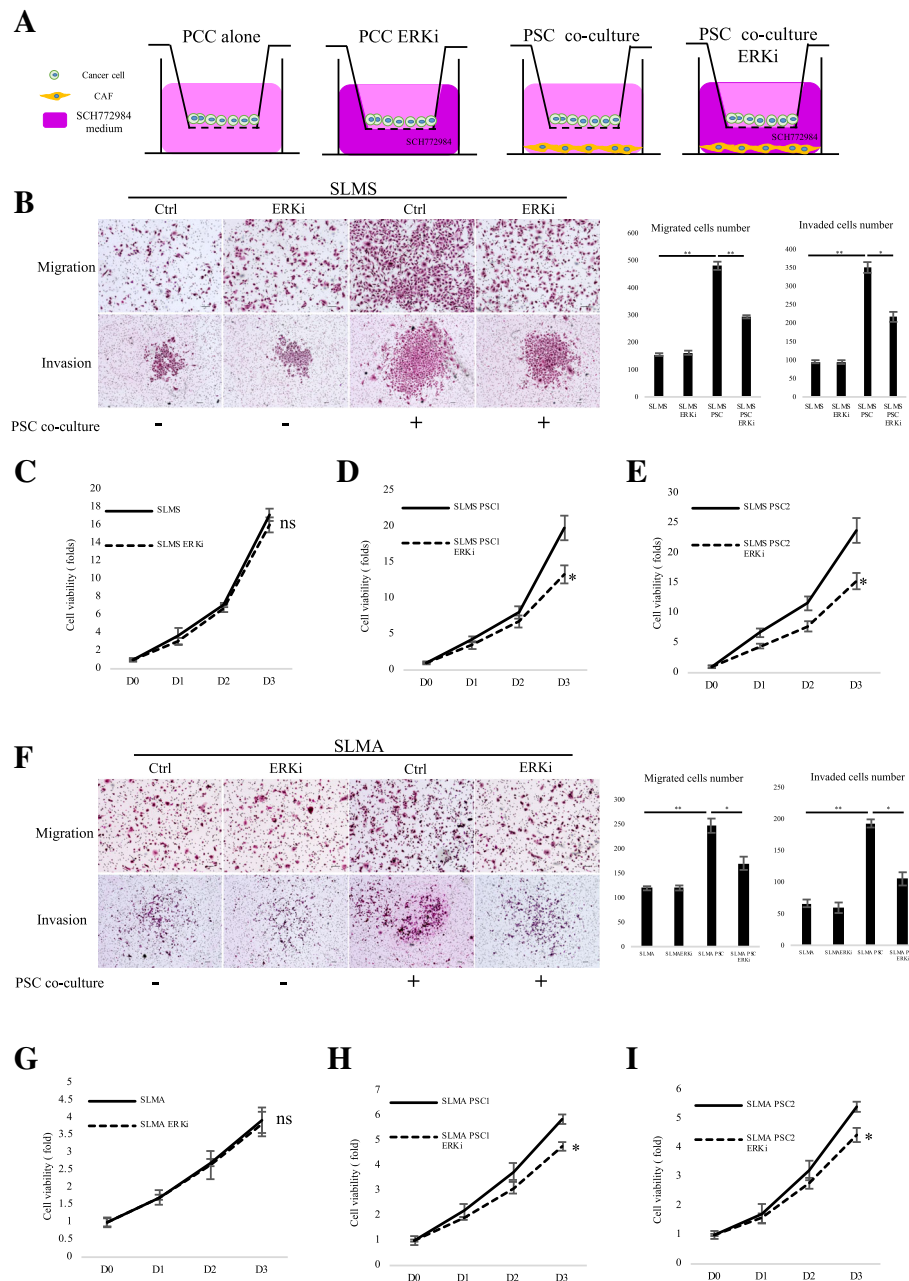


**Fig. 5** Inhibition of ERK1/2 suppressed PCC-PSC interaction by preferentially targeting PSC. **a** In indirect co-culture experiments, first PSCs were seeded, and 24 h later, medium was replaced and transwell chambers (8- $\mu$ m pores; Becton Dickinson) were placed in 24-well dishes, and then PCCs were seeded into the transwell chambers. After incubation for the indicated time, migration and invasion were evaluated by counting the cells that had invaded to the lower chamber. SCH772984 dose was used IC50 value of PSC2 cells, 89 nM. **b** Migration and invasion assays were performed for 18 and 36 h, respectively. Graphs show numbers of cells calculated from five fields. Scale bars = 100  $\mu$ m. \* $P$  < 0.05, \*\* $P$  < 0.01. **c** Viability of SLMS cells co-cultured with **(d)** PSC1 or **(e)** PSC2 cells after DMSO or SCH772984 treatment; **(g)** Viability of SLMA cells co-cultured with **(h)** PSC1 or **(i)** PSC2 cells after DMSO or SCH772984 treatment was determined by CellTiter-Glo luminescent cell viability assay. SCH772984 dose was used IC50 value of PSC1, 321 nM; and PSC2, 90 nM. \* $P$  < 0.05. Columns, mean fold changes of three experiments done in triplicate

However, this lower dose of SCH772984 inhibited PCC migration and invasion when co-cultured with PSCs (Fig. 5b, f). In addition, a direct co-culture cell viability assay revealed SCH772984 suppressed

proliferation of PCCs and PSCs co-cultured at the lower PSC IC50 dose (Fig. 5c-e and g-i). However, we did not obtain a similar finding for monocultured PCCs. These results suggest that treatment with

SCH772984 could preferentially target PSCs to suppress cancer–stromal interaction.

#### **Combining SCH772984 with CQ suppressed fibrosis and induced senescence in PSCs**

To evaluate therapeutic efficiency, we combined SCH772984 with an effective autophagy inhibitor CQ, which is shown to suppress PSCs activation via inhibition of autophagy activity [23]. A further morphology change was observed in PSCs after the combined treatment (Fig. 6a; Additional file 3: Figure S3a). Compared with a 4-fold increase in viability of control PSCs, the combined treatment remarkably restricted proliferation of PSCs (Fig. 6b; Additional file 3: Figure S3b); It also down-regulated  $\alpha$ -SMA and Collagen Type I expression, and up-regulated senescence markers p15 and p16, compared with SCH772984 treatment alone (Fig. 6c; Additional file 3: Figure S3c). Primary cultured PSCs partly exhibited positive beta-galactosidase staining as shown in the previous reports [37]. We performed senescence  $\beta$ -galactosidase staining to investigate the correlation between p15/p16 expression and autophagy during PSC cellular senescence. We found SCH772984 treatment did not increase cellular senescence in PSCs, possibly due to autophagy activation, although p15/p16 expression was up-regulated, and combined SCH772984 + CQ remarkably induced PSC cellular senescence (Fig. 6d; Additional file 3: Figure S3d). Therefore, combining SCH772984 with CQ suppressed drug-induced autophagy of SCH772984 and led to cellular senescence in PSCs.

#### **Combining SCH772984 with CQ suppressed cell viability and induced apoptosis in PCCs**

Next, we evaluated the therapeutic effect of combine treatment of SCH772984 with CQ in PCCs. Single agent and/or combine treatment of SCH772984 and CQ didn't affect the migration capacity of PCCs. SCH772984, but not CQ, significantly suppressed invasion of PCCs. And this effect was not further promoted by combine treatment with CQ. However, this effect was not further promoted by combine treatment with CQ (Fig. 6e; Additional file 3: Figure S3e). In addition, cell viability of PCCs was significantly suppressed by single agent of ERK inhibitor or CQ, and combination treatment further suppressed cell viability compared to single agent (Fig. 6f; Additional file 3: Figure S3f). Furthermore, the EMT transition was downregulated of PCCs following SCH772984 alone treatment and/or combination treatment. PCCs didn't upregulated the cellular senescence markers p15 and p16 unlike PSCs. Instead, we observed an induction of CC8 expression, indicating combination treatment induced significant apoptosis of PCCs (Fig. 6g; Additional file 3: Figure S3g).

#### **Combination of SCH772984 and CQ inhibited metastases in KPC cancer organoid xenograft mouse model**

ERK1/2 inhibitor was identified as a potential therapeutic agent for primary liver cancer in organoid xenograft experiments [38]. A pancreatic tumor organoid was shown to recapitulate the histology and gene expression of its parental tumor [25, 39]. We therefore generated cancer organoids for 2 weeks using KPC-derived PDAC cells as described previous (Fig. 7a) [21]. Organoid or 2D-cultured cells were then splenic transplanted into nude mice with KPC-derived PSCs. Consistent with previous reports [17, 32], SCH772984 treatment did not cause any toxic effects such as body weight loss. Compared to 2D-cultured cells, there was no significant increase of liver metastasis in splenic xenograft experiment using organoid. However, the implanted tumor derived from organoids frequently restored high p-ERK1/2 expression, which was consistent with the original tumor (Additional file 4: Figure S4). Because of these results, we chose organoid xenografts for the following experiments. KPC cancer organoids were splenic co-transplanted into nude mice with KPC-derived PSCs. One week after implantation, mice were treated intraperitoneally with either vehicle, SCH772984, CQ or combination according to the dosing schedule indicated in the figure legends (Fig. 7b). After 13 days of treatment, their liver metastases were harvested and evaluated (Fig. 7c). Compared with controls, the combined treatment group remarkably decreased the metastatic nodules (14 vs. 2, average) in the liver (Fig. 7d), liver volume (2.53 vs. 1.29cm<sup>3</sup>, average) and liver weight (1.65 g vs. 1.29 g, average), although SCH772984 alone and CQ alone also decreased metastatic nodules (14 vs. 5, 14 vs. 6, average) (Fig. 7e, f). Histologic analysis by using serial sections demonstrated that Ki67 expression was downregulated in the combined treatment (6% positive) group compared with control (44% positive) group and/or single-agent treatment (18% positive for SCH772984 and 36% positive for CQ) groups (Fig. 7g). The corresponding rectangles indicated reduction of p-ERK1/2 expression in  $\alpha$ -SMA-positive PSCs compared with controls. In addition, masson's trichrome stain demonstrated significant decrease in the expression of collagen fibers (7% positive) in combined treatment group compared with control (12% positive) group and/or single-agent treatment (22% positive for SCH772984 and 14% positive for CQ) groups (Fig. 7g).

#### **Discussion**

In the present study, we investigated p-ERK1/2 expression in PCCs and PSCs, and its functional impact on pancreatic cancer–stromal interaction. Our results showed that ERK1/2 activation is upregulated during PCC metastasis and PCC–PSC interaction. Inhibition of p-ERK1/2 in PCCs and PSCs induced remarkable cell viability repression and changes in mRNA

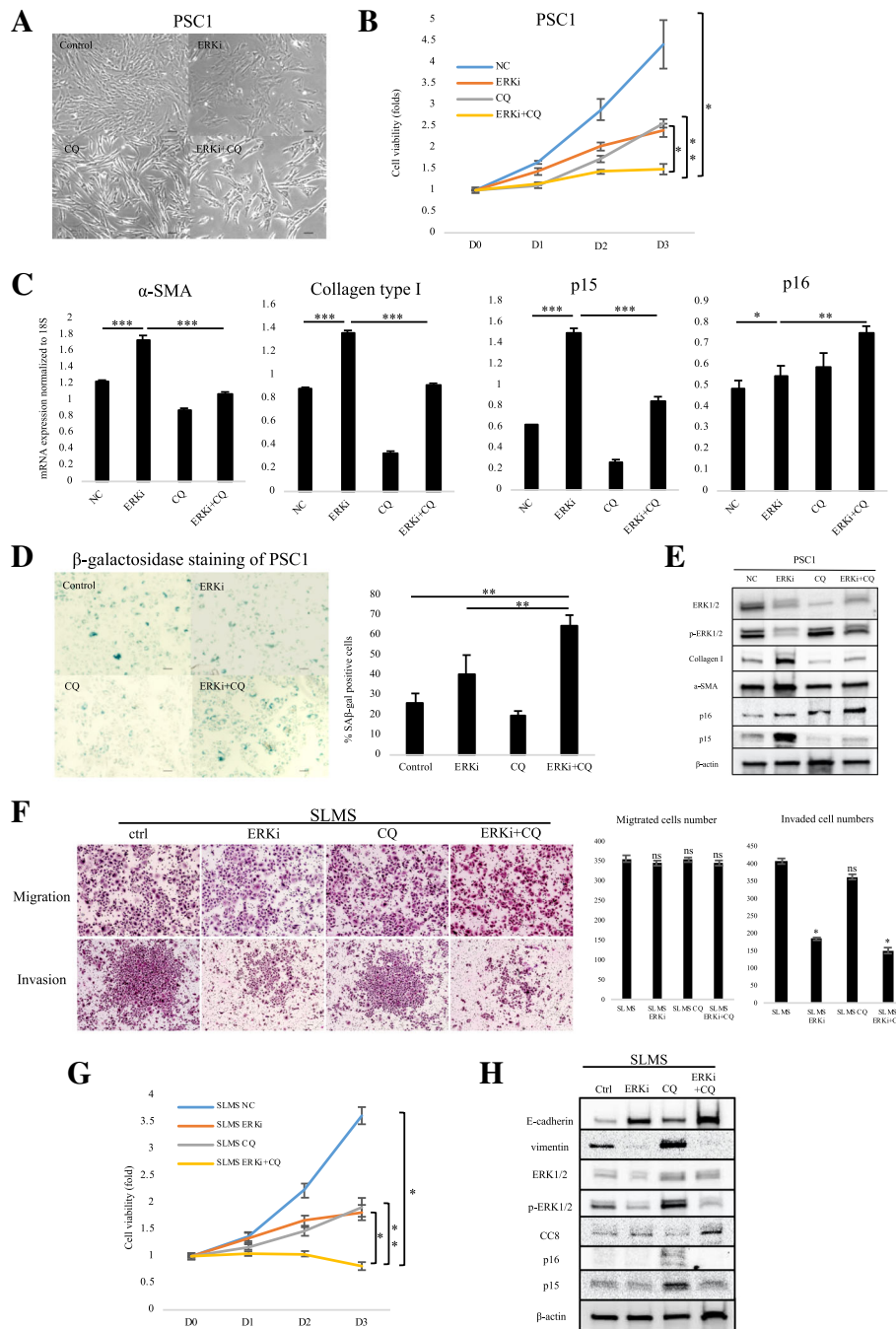


**Fig. 6** Dual treatment of SCH772984 and CQ decreased cell viability and induced senescence of PSCs. **a** Western blot of fibronectin,  $\alpha$ -SMA, LC3-II, Akt and p-Akt levels of PSCs after treatment with ERK inhibitor. **b** Microphotograph of PSCs after indicated agent treatment. Scale bars = 100  $\mu$ m. **c** Cell viability of PSCs after indicated agent treatment. **d** qRT-PCR shows mRNA expression of  $\alpha$ -SMA, Collagen Type I, p15 and p16. \* $P$  < 0.05, \*\* $P$  < 0.01, \*\*\* $P$  < 0.001. **e**  $\beta$ -galactosidase staining of PSCs after indicated agent treatment. Bottom: graphs show the quantification of  $\beta$ -gal-positive cells calculated from five fields. Scale bars = 100  $\mu$ m. \* $P$  < 0.05. **e** Migration and invasion assays were performed for 18 and 36 h, respectively. Graphs show numbers of cells calculated from five fields. Scale bars = 100  $\mu$ m. \* $P$  < 0.05. **f** Cell viability of PCCs after indicated agent treatment. Columns, mean fold changes in three experiments done in triplicate. **g** Western blot of indicated protein levels in PCCs after indicated treatment

expression. Delivery of ERK inhibitor repressed cancer-stromal interaction via a PSC-preferential behavior. We also found ERK inhibition to induce

autophagy in PSCs, and this effect was suppressed by combining the ERK inhibitor with the autophagy inhibitor, CQ (Fig. 8).

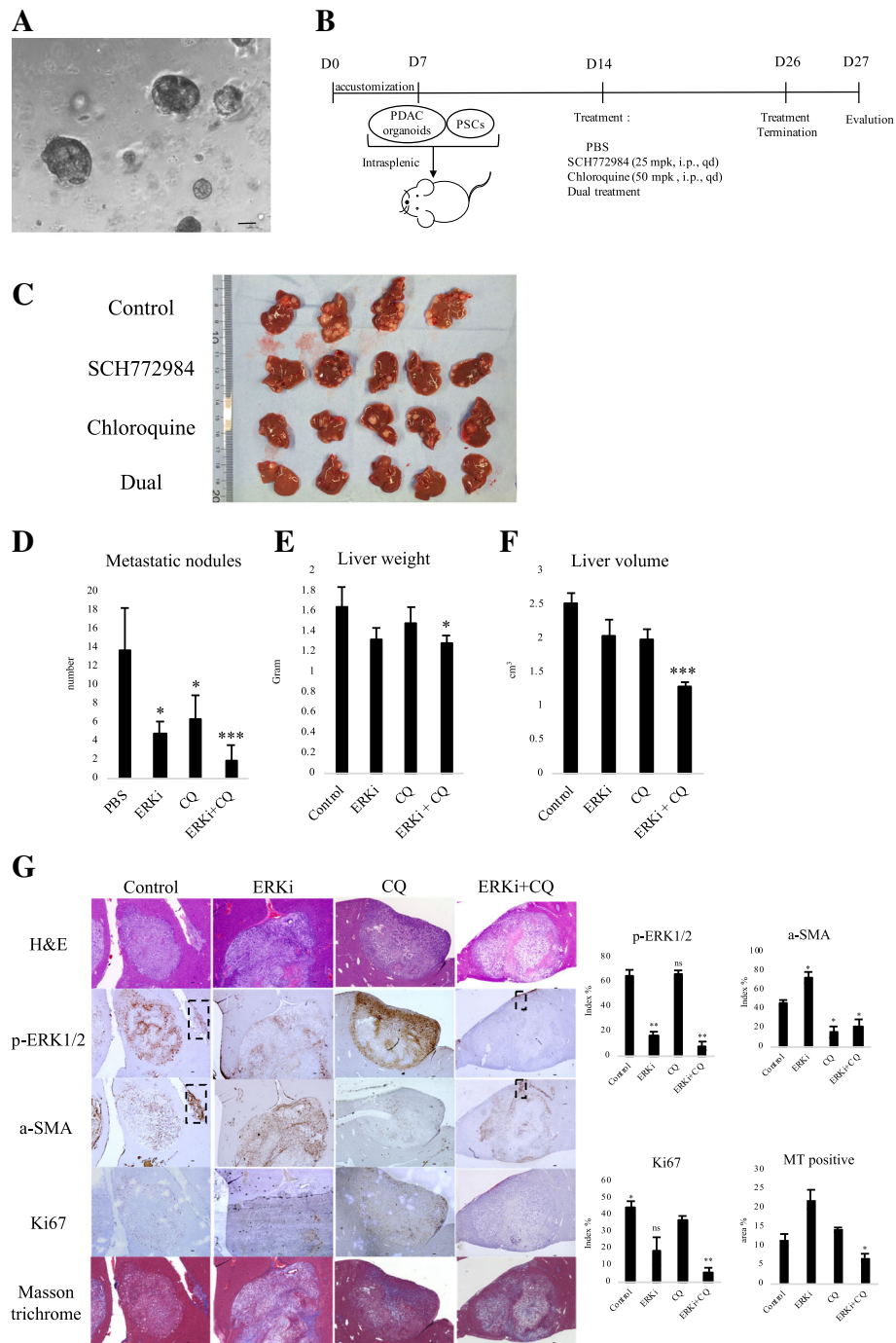
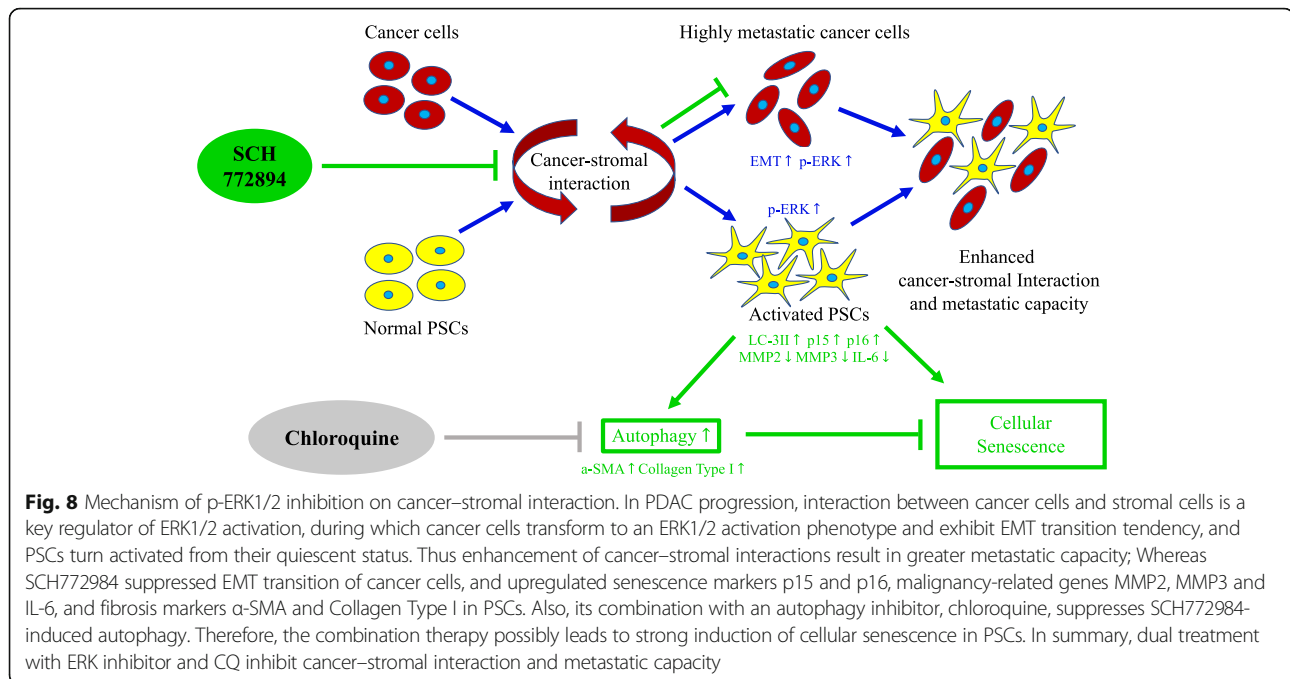


**Fig. 7** Dual treatment of SCH772984 and CQ decreased liver metastasis in xenograft organoid model with PSC co-transplantation. **a** Microphotograph of KPC mouse-derived cancer organoid. Scale bars =100 μm. **b** Scheme of xenograft experiment. Female nude mice were intrasplenic transplanted with cancer organoids with PSCs and randomized divided into four groups (n = 5/group). One week after implantation, mice were dosed once daily with vehicle, SCH772984 (25 mg/kg), Chloroquine (50 mg/kg), or dual treatment of each group for 13 days. Dosing occurred from day 14 to day 26. At day 27, mice were sacrificed and liver metastases were harvested. **c** Gross pathology showed significantly reduced liver metastasis formation after dual treatment of SCH772984 with chloroquine. **d** Liver metastasis nodules were significantly reduced in samples treated with SCH772984 or CQ, or both. \*P < 0.05, \*\*\*P < 0.001. **e** Tumor weight and **(f)** volume were significantly decreased only in the dual-treatment group. \*P < 0.05, \*\*\*P < 0.001. **g** Immunohistochemical staining shows decreased p-ERK1/2 expression in SCH772984 group, and decreased α-SMA expression in CQ group; The dual-treated group showed significant reductions of p-ERK1/2, α-SMA, Ki67 and collagen fibers. Corresponding rectangles indicated α-SMA-positive PSCs. Right: quantification of gene expression from five fields. Scale bars =100 μm. \*P < 0.05, \*\*P < 0.01



Previous studies have focused mainly on the RAS-RAF-MEK-ERK pathway in cancer cells. However, p-ERK1/2 expression has been shown prognostic and metastatic implications in PDAC [40, 41]. Our result showed HMPDAC cells had high levels of activated ERK1/2, whereas inhibiting ERK1/2 suppressed EMT in these cells. Furthermore, activation of ERK1/2 also increased in PDAC cells after co-culture with PSCs. These findings indicate that activation of ERK1/2 promotes metastasis and cancer–stromal interaction in PDAC cells. We found that activation of ERK1/2 was frequently observed in stroma even compared with PCCs in the resected pancreatic cancer tissues. Moreover, cancer-associated PSCs were more sensitive to ERK inhibitor SCH772984 than cancer cells. Therefore, the present research focused on the activation of ERK1/2 in PSCs as well as PCCs. Cancer-associated PSCs are the major components of extensive desmoplasia, which contribute to PDAC progression and chemoresistance [42]. Recently, anti-stromal drugs were reported to inhibit PDAC progression via suppression of PSCs [43, 44]. These findings suggest that inhibiting PSCs could be the basis of an effective therapeutic strategy for PDAC.

Inhibition of ERK pathway increased sensitization to gemcitabine of PDAC cells and PDAC xenograft mouse model [43]. The present data demonstrated that ERK inhibitor improved chemosensitivity of gemcitabine of PDAC cells in the PSC-conditioned medium. However, our results suggest that inhibiting ERK1/2 is a two-edged sword that simultaneously induces autophagy and suppresses cell viability in PSCs. Autophagy in

PDAC stroma is associated with accelerated cancer progression; high expression of LC3-II, an autophagy marker, in PDAC specimens is prognostic of poor survival [23]. Immunohistochemical analysis of mouse fibroblasts revealed increased co-localization of p-ERK1/2 with LC3-II and Autophagy-related proteins such as Atg5, Atg12 and Atg16 [45]. Cytoplasmic sequestration of ERK1/2 has been shown to promote autophagy in human ovarian cancer cells [46]. However, autophagy prevents cellular senescence [47]. Therefore, ERK1/2 inhibition did not induce senescence in PSCs, despite increased expression of p15 and p16. The protein p16 is a major player in cellular response to DNA damage, which leads to senescence [48] and/or apoptosis [49, 50]. Overexpression of p16 activates autophagy and cellular senescence in both human fibroblasts and breast cancer cells [51]. However, the mechanism of ERK inhibitor-induced autophagy is unclear. Although further investigation is needed, it may be initiated by p16-induced DNA damage, which upregulates p53; p53 then activates transcription of several autophagy-related genes including *ATG5* and *ATG7* [52]. As inhibition of autophagy induces cellular senescence in primary human fibroblasts [53], we chose CQ as our combination drug, thus we obtained a satisfactory result.

Tumor organoid models are a new tool in biomedical research, and have been recently used to explore the effects of p-ERK1/2 inhibitors on several types of cancer, including ERK inhibitor SCH772984 in hepatocellular carcinoma [38] and bladder cancer [54]. SCH772984 also suppressed formation and viability of patient-derived

pancreatic organoids [55]. In the present study, we performed *in vivo* xenograft experiment using patient-derived PDAC organoids, and found that ERK inhibitor treatment alone reduced the number of metastatic nodules and Ki67 expression in liver metastases. Compared to 2D-adherent cultured cells, pancreatic cancer organoids demonstrated greater p-ERK1/2 expression, which was consistent with the findings in original resected PDAC tumors, and suggests that organoid models can be used to investigate the therapeutic effects of ERK inhibitors, due to the reproducible p-ERK1/2 expression, which is consistent with that in resected samples.

## Conclusion

In summary, inhibition of p-ERK1/2 preferentially suppressed cancer–stromal interaction by decreasing viability of PSCs. However, ERK inhibitor also induced autophagy and may have prevented senescence of the activated PSCs. Our findings also indicate that combined inhibition of ERK1/2 and autophagy significantly decreased the number, volume and weight of liver metastases. Taken together, combination therapy to suppress ERK1/2 and autophagy is a potential treatment for pancreatic cancer.

## Additional files

**Additional file 1: Figure S1.** Characteristics of highly metastatic PDAC cells. (A) Suspended cell viability of cancer cells as determined by CellTiter-Glo luminescent cell viability assay.  $**P < 0.01$ . (B) Tumor weight but not volume was significantly increased in dual-treatment group.  $*P < 0.05$ . (C) SLMS/SUIT-2 ratio for protein kinases expression of significance. (D) Western blot of ERK1/2, p-ERK1/2, E-cadherin and vimentin levels in highly metastatic and parental PDAC cells. (PDF 262360 kb)

**Additional file 2: Figure S2.** Expression and prognosis of p-ERK1/2 in PDAC database. (A) ERK1 and (B) ERK2 expression was detected in both cancer and stromal cells in human pancreatic primary tumor. (C, D) Kaplan–Meier survival analysis of overall survival and disease-free survival of patients with pancreatic cancer by *ERK1* and *ERK2* mRNA expression. (PDF 262364 kb)

**Additional file 3: Figure S3.** Dual-treatment with SCH772984 and CQ decreased cell viability and induced PSC2 senescence. (A) Microphotograph of PSC2 cells after treatment with indicated agents. Scale bars = 100  $\mu$ m. (B) Viability of PSCs after treatment with indicated agents. (C) qRT-PCR showed mRNA expression of  *$\alpha$ -SMA*, Collagen Type I, *p15* and *p16*.  $*P < 0.05$ ,  $**P < 0.01$ ,  $***P < 0.001$ . (D)  $\beta$ -galactosidase staining of PSC2 cells after treatment with indicated agents. Graphs show the quantification of  $\beta$ -gal-positive cells calculated from five fields. Scale bars = 100  $\mu$ m.  $*P < 0.05$ . (E) Migration and invasion assays were performed for 18 and 36 h, respectively. Graphs show numbers of cells calculated from five fields. Scale bars = 100  $\mu$ m.  $*P < 0.05$ . (F) Cell viability of PCCs after indicated agent treatment. Columns, mean fold changes of three experiments done in triplicate. (G) Western blot of indicated protein levels of PCCs after indicated treatment. (PDF 262364 kb)

**Additional file 4: Figure S4.** Pancreatic tumor organoid recapitulates p-ERK1/2 expression of PDAC *in vitro* and *in vivo*. (A) Western blot of ERK1/2 and p-ERK1/2 shows increasing p-ERK1/2 level in KPC cancer organoid compared with cancer cells. (B) Scheme of xenograft experiment. Mice were randomly divided into two groups and  $5 \times 10^4$  cancer cells or organoids were intrasplenic implanted with  $5 \times 10^4$  PSCs. After 2 weeks, liver metastases were evaluated. (C) H&E staining and immunohistochemical

staining show metastatic nodules (D), and expression of  $\alpha$ -SMA (E) and p-ERK1/2 (F). (G, H) Combination of indicated dose of SCH772984 improved chemosensitivity of gemcitabine of AsPC-1 and SUIT-2 cells in the PSC-conditioned medium. Columns, mean fold changes of three experiments done in triplicate. (PDF 262364 kb)

**Additional file 5: Table S1.** Primers used for quantitative RT-PCR. (DOCX 56 kb)

**Additional file 6: Table S2.** Clinicopathological features of PADAC samples used for p-ERK1/2 immunohistochemistry. (XLSX 11 kb)

## Abbreviations

CQ: chloroquine; EMT: epithelial–mesenchymal transition; ERK: Extracellular signal-regulated kinases; HM: highly metastatic; HMPCC: highly metastatic pancreatic cancer cell; HPDE: Human pancreatic ductal epithelial; IC50: 50% inhibitory concentration; KPC: LSL-Kras G12D/+; LSL: Trp53R172H/+; MAPK: Mitogen-activated protein kinases; OS: overall survival; PCC: pancreatic cancer cell; PDAC: Pancreatic ductal adenocarcinoma; Pdx: 1-Cre; PSC: pancreatic stellate cell

## Acknowledgements

We are grateful to Emiko Manabe and Shoko Sadatomi (Department of Surgery and Oncology, Kyushu University) for their skillful technical assistance. Zilong Yan is the recipient of Rotary Yoneyama Memorial Foundation scholarship [<http://www.rotary-yoneyama.or.jp>]. We also thank Marla Brunker, from Edanz Group ([www.edanzediting.com/ac](http://www.edanzediting.com/ac)) for editing a draft of this manuscript.

## Funding

This work was supported by JSPS KAKENHI (Grant numbers: 26108010, 26293305, 15 K10185, 25713050, 16 K15621, 16 K10601, 16 K10600, 16H05417, 15 K15498, 15H04933, 16H05418, 17H04284, 17 K19602 and 17 K19605).

## Availability of data and materials

All data generated or analyzed during this study are included either in this article or in the supplementary information files.

## Authors' contributions

ZY designed the study, conducted experiments, acquired and analyzed data, and wrote the manuscript. SF, BZ, WG, HF, SK, YA, KK, TA, CI, KS, TM, KN, YM, TO, KM and MH discussed and revised the manuscript; KO, MN was responsible for the conception and supervision of the study and wrote the manuscript. All authors corrected drafts and approved the final version of the manuscript.

## Ethics approval and consent to participate

This study was approved by the Kyushu University Institutional Review Board (Fukuoka, Japan). All patients studied signed an informed consent for participation. All animal procedures and care were conducted in accordance with institutional guidelines and in compliance with national and international laws and policies.

## Consent for publication

Not applicable.

## Competing interests

The authors declare that they have no competing interests.

## Publisher's Note

Springer Nature remains neutral with regard to jurisdictional claims in published maps and institutional affiliations.

## Author details

<sup>1</sup>Department of Surgery and Oncology, Graduate School of Medical Sciences, Kyushu University, 3-1-1 Maidashi, Fukuoka 812-8582, Japan. <sup>2</sup>Department of Advanced Medical Initiatives, Graduate School of Medical Sciences, Kyushu University, Fukuoka, Japan. <sup>3</sup>Department of General Surgery, Shenzhen University General Hospital, Shenzhen, China. <sup>4</sup>Cancer Center of Kyushu University Hospital, Fukuoka, Japan.

Received: 13 February 2019 Accepted: 10 May 2019

Published online: 27 May 2019

## References

- Stewart BW, Wild CP. World cancer report 2014. World Heal Organ [Internet]. 2014;1–2. Available from: [https://www.who.int/cancer/publications/WRC\\_2014/en/](https://www.who.int/cancer/publications/WRC_2014/en/).
- Hess KR, Varadhachary GR, Taylor SH, Wei W, Raber MN, Lenzi R, et al. Metastatic patterns in adenocarcinoma. *Cancer*. 2006;106:1624–33.
- Howlader N, Noone AM, Krapcho M et al. SEER Cancer Statistics Review, 1975–2013. Natl Cancer Institute Bethesda, MD [Internet]. 2016. Available from: [http://seer.cancer.gov/csr/1975\\_2013/](http://seer.cancer.gov/csr/1975_2013/).
- Gleisner AL, Assumpcao L, Cameron JL, Wolfgang CL, Choti MA, Herman JM, et al. Is resection of periampullary or pancreatic adenocarcinoma with synchronous hepatic metastasis justified? *Cancer*. 2007;110:2484–92.
- Neesse A, Michl P, Frese KK, Feig C, Cook N, Jacobetz MA, et al. Stromal biology and therapy in pancreatic cancer. *Gut*. 2011.
- Minchinton AI, Tannock IF. Drug penetration in solid tumours. *Nat Rev Cancer*. 2006.
- Apte MV, Haber PS, Applegate TL, Norton ID, McCaughan GW, Korsten MA, et al. Periacinar stellate shaped cells in rat pancreas: identification, isolation, and culture. *Gut*. 1998.
- Apte MV, Haber PS, Darby SJ, Rodgers SC, McCaughan GW, Korsten MA, et al. Pancreatic stellate cells are activated by proinflammatory cytokines: implications for pancreatic fibrogenesis. *Gut*. 1999.
- Whatcott CJ, Diep CH, Jiang P, Watanabe A, Lobello J, Sima C, et al. Desmoplasia in primary tumors and metastatic lesions of pancreatic cancer. *Clin Cancer Res*. 2015;21:3561–8.
- McCubrey JA, Steelman LS, Chappell WH, Abrams SL, Wong EWT, Chang F, et al. Roles of the Raf/MEK/ERK pathway in cell growth, malignant transformation and drug resistance. *Biochim Biophys Acta - Mol Cell Res*. 2007;1773:1263–84.
- Bartholomeusz C, Gonzalez-Angulo AM, Liu P, Hayashi N, Lluch A, Ferrer-Lozano J, et al. High ERK protein expression levels correlate with shorter survival in triple-negative breast cancer patients. *Oncologist*. 2012.
- Virtakoivu R, Mai A, Mattila E, De Franceschi N, Imanishi SY, Corthals G, et al. Vimentin-ERK signaling uncouples slug gene regulatory function. *Cancer Res*. 2015.
- Ng KY, Chan LH, Chai S, Tong M, Guan XY, Lee NP, et al. TP53INP1 downregulation activates a p73-dependent DUSP10/ERK signaling pathway to promote metastasis of hepatocellular carcinoma. *Cancer Res*. 2017.
- Yu Y, Luk F, Yang JL, Walsh WR. Ras/Raf/MEK/ERK pathway is associated with lung metastasis of osteosarcoma in an orthotopic mouse model. *Anticancer Res*. 2011;31:1147–52.
- Ai X, Wu Y, Zhang W, Zhang Z, Jin G, Zhao J, et al. Targeting the ERK pathway reduces liver metastasis of Smad4-inactivated colorectal cancer. *Cancer Biol Ther*. 2013;14:1059–67.
- Principe DR, Diaz AM, Torres C, Mangan RJ, DeCant B, McKinney R, et al. TGF $\beta$  engages MEK/ERK to differentially regulate benign and malignant pancreas cell function. *Oncogene* [internet]. Nat Publ Group; 2017;36:4336–48. Available from: <http://www.nature.com/doi/10.1038/onc.2016.500>.
- Hayes TK, Neel NF, Hu C, Gautam P, Chenard M, Long B, et al. Long-term ERK inhibition in KRAS-mutant pancreatic Cancer is associated with MYC degradation and senescence-like growth suppression. *Cancer cell* [Internet]. Elsevier Inc.; 2016;29:75–89. Available from: <https://doi.org/10.1016/j.ccell.2015.11.011>
- Hingorani SR, Wang L, Multani AS, Combs C, Deramautd TB, Hruban RH, et al. Trp53R172H and KrasG12D cooperate to promote chromosomal instability and widely metastatic pancreatic ductal adenocarcinoma in mice. *Cancer Cell*. 2005.
- Bachem MG, Schünemann M, Ramadani M, Siech M, Beger H, Buck A, et al. Pancreatic carcinoma cells induce fibrosis by stimulating proliferation and matrix synthesis of stellate cells. *Gastroenterology*. 2005.
- Bachem MG, Schneider E, Groß H, Weidenbach H, Schmid RM, Menke A, et al. Identification, culture, and characterization of pancreatic stellate cells in rats and humans. *Gastroenterology*. 1998.
- Koikawa K, Ohuchida K, Ando Y, Kibe S, Nakayama H, Takesue S, et al. Basement membrane destruction by pancreatic stellate cells leads to local invasion in pancreatic ductal adenocarcinoma. *Cancer Lett*. 2018.
- Ikenaga N, Ohuchida K, Mizumoto K, Cui L, Kayashima T, Morimatsu K, et al. CD10+ pancreatic stellate cells enhance the progression of pancreatic cancer. *Gastroenterology* [Internet]. Elsevier Inc.; 2010;139:1041–1051.e8. Available from: <https://doi.org/10.1053/j.gastro.2010.05.084>
- Endo S, Nakata K, Ohuchida K, Takesue S, Nakayama H, Abe T, et al. Autophagy Is Required for Activation of Pancreatic Stellate Cells, Associated With Pancreatic Cancer Progression and Promotes Growth of Pancreatic Tumors in Mice. *Gastroenterology*. Elsevier, Inc; 2017;152:1492–1506.e24.
- Ohuchida K, Mizumoto K, Murakami M, Qian LW, Sato N, Nagai E, et al. Radiation to stromal fibroblasts increases invasiveness of pancreatic Cancer cells through tumor-stromal interactions. *Cancer Res*. 2004;64:3215–22.
- Boj SF, IL HC, Baker LA, Chio IIC, Engle DD, Corbo V, et al. Organoid models of human and mouse ductal pancreatic cancer. *Cell*. 2015;160:324–38.
- Chijiwa Y, Moriyama T, Ohuchida K, Nabae T, Ohtsuka T, Miyasaka Y, et al. Overexpression of microRNA-5100 decreases the aggressive phenotype of pancreatic cancer cells by targeting PODXL. *Int J Oncol*. 2016;48:1688–700.
- Zheng B, Ohuchida K, Chijiwa Y, Zhao M, Mizuuchi Y, Cui L, et al. CD146 attenuation in cancer-associated fibroblasts promotes pancreatic cancer progression. *Mol Carcinog*. 2016;55:1560–72.
- Gao J, Aksoy BA, Dogrusoz U, Dresdner G, Gross B, Sumer SO, et al. Integrative analysis of complex cancer genomics and clinical profiles using the cBioPortal. *Sci Signal*. 2013.
- Cerami E, Gao J, Dogrusoz U, Gross BE, Sumer SO, Aksoy BA, et al. The cBio Cancer genomics portal: an open platform for exploring multidimensional cancer genomics data. *Cancer Discov*. 2012.
- Mahadevan D, Von Hoff DD. Tumor-stroma interactions in pancreatic ductal adenocarcinoma. *Mol Cancer Ther* [Internet]. 2007;6:1186–97. Available from: <http://mct.aacrjournals.org/cgi/doi/10.1158/1535-7163.MCT-06-0686>.
- Kikuta K, Masamune A, Watanabe T, Ariga H, Itoh H, Hamada S, et al. Pancreatic stellate cells promote epithelial-mesenchymal transition in pancreatic cancer cells. *Biochem Biophys Res Commun* [Internet]. 2010;403:380–4. Available from: <http://www.sciencedirect.com/science/article/pii/S0006291X1002098X>.
- Morris EJ, Jha S, Restaino CR, Dayananth P, Zhu H, Cooper A, et al. Discovery of a novel ERK inhibitor with activity in models of acquired resistance to BRAF and MEK inhibitors. *Cancer Discov*. 2013;3:742–50.
- Javle MM, Gibbs JF, Iwata KK, Pak Y, Rutledge P, Yu J, et al. Epithelial-mesenchymal transition (EMT) and activated extracellular signal-regulated kinase (p-Erk) in surgically resected pancreatic cancer. *Ann Surg Oncol*. 2007.
- Ikenaga N, Ohuchida K, Mizumoto K, Cui L, Kayashima T, Morimatsu K, et al. CD10+pancreatic stellate cells enhance the progression of pancreatic cancer. *Gastroenterology*. 2010;139:1041–51.
- Coppé J, Rodier F, Patil CK, Freund A, Desprez P, Campisi J. Tumor suppressor and aging biomarker p16 INK4a induces cellular senescence without the associated inflammatory secretory phenotype \*  $\square$ . 2011;286:36396–403.
- Vijayaraghavan S, Karakas C, Doostan I, Chen X, Bui T, Yi M, et al. CDK4/6 and autophagy inhibitors synergistically induce senescence in Rb positive cytoplasmic cyclin E negative cancers. *Nat Commun* [Internet]. Nat Publ Group. 2017;8:15916. Available from: <http://www.ncbi.nlm.nih.gov/pubmed/28653662>.
- Wang T, Notta F, Navab R, Joseph J, Ibrahimov E, Xu J, et al. Senescent carcinoma-associated fibroblasts upregulate IL8 to enhance Prometastatic phenotypes. *Mol Cancer Res*. 2017.
- Broutier L, Mastrogianni G, Versteegen MMA, Francies HE, Gavarró LM, Bradshaw CR, et al. Human primary liver cancer-derived organoid cultures for disease modeling and drug screening. *Nat Med*. 2017;23:1424–35.
- Huang L, Holtzinger A, Jagan I, Begora M, Lohse I, Ngai N, et al. Ductal pancreatic cancer modeling and drug screening using human pluripotent stem cell- and patient-derived tumor organoids. *Nat Med*. 2015.
- Chadha KS, Khoury T, Yu J, Black JD, Gibbs JF, Kuvshinov BW, et al. Activated Akt and Erk expression and survival after surgery in pancreatic carcinoma. *Ann Surg Oncol*. 2006.
- Yan Z, Ohuchida K, Zheng B, Okumura T, Takesue S, Nakayama H, et al. CD110 promotes pancreatic cancer progression and its expression is correlated with poor prognosis. *J Cancer Res Clin Oncol* [Internet]. Springer Berlin Heidelberg; 2019;145:1147–64. Available from: <https://doi.org/10.1007/s00432-019-02860-z>
- Pandol S, Edderkaoui M, Gukovsky I, Lugea A, Gukovskaya A. Desmoplasia of pancreatic ductal adenocarcinoma. *Clin Gastroenterol Hepatol*. 2009.
- Kozono S, Ohuchida K, Eguchi D, Ikenaga N, Fujiwara K, Cui L, et al. Pirfenidone inhibits pancreatic cancer desmoplasia by regulating stellate cells. *Cancer Res*. 2013;73:2345–56.

44. Yoshida M, Miyasaka Y, Ohuchida K, Okumura T, Zheng B, Torata N, et al. Calpain inhibitor calpeptin suppresses pancreatic cancer by disrupting cancer – stromal interactions in a mouse xenograft model. 2016;107.
45. Martinez-Lopez N, Athonvarangkul D, Mishall P, Sahu S, Singh R. Autophagy proteins regulate ERK phosphorylation. *Nat Commun* [Internet]. Nat Publ Group; 2013;4:2799. Available from: <http://www.nature.com/ncomms/2013/131118/ncomms3799/full/ncomms3799.html#f4>.
46. Bartholomeusz C, Rosen D, Wei C, Kazansky A, Yamasaki F, Takahashi T, et al. PEA-15 induces autophagy in human ovarian cancer cells and is associated with prolonged overall survival. *Cancer Res*. 2008.
47. García-Prat L, Martínez-Vicente M, Perdiguero E, Ortet L, Rodríguez-Ubreva J, Rebollo E, et al. Autophagy maintains stemness by preventing senescence. *Nature*. 2016;
48. Collado M, Serrano M. Senescence in tumours: evidence from mice and humans. *Nat Rev Cancer* [Internet]. Nat Publ Group; 2010;10:51–7. Available from: <https://doi.org/10.1038/nrc2772><http://www.nature.com/nrc/journal/v10/n1/pdf/nrc2772.pdf>
49. Mirzayans R, Andrais B, Hansen G, Murray D. Role of p16 INK4A in replicative senescence and DNA damage-induced premature senescence in p53-deficient human cells. *Biochem Res Int*. 2012;2012.
50. Rayess H, Wang MB, Srivatsan ES. Cellular senescence and tumor suppressor gene p16. *Int J Cancer*. 2012.
51. Capparelli C, Guido C, Whitaker-Menezes D, Bonuccelli G, Balliet R, Pestell TG, et al. Autophagy and senescence in cancer-associated fibroblasts metabolically supports tumor growth and metastasis, via glycolysis and ketone production. *Cell Cycle*. 2012.
52. White E. Autophagy and p53. *Cold Spring Harb Perspect Med*. 2016.
53. Kang HT, Lee KB, Kim SY, Choi HR, Park SC. Autophagy impairment induces premature senescence in primary human fibroblasts. *PLoS One*. 2011.
54. Lee SH, Hu W, Matulay JT, Silva MV, Owczarek TB, Kim K, et al. Tumor evolution and drug response in patient-derived organoid models of bladder Cancer. *Cell*. 2018.
55. Del CA, Conciatori F, Incani UC, Bazzichetto C, Falcone I, Corbo V, et al. Therapeutic potential of combined BRAF / MEK blockade in BRAF -wild type preclinical tumor models. *J Exp Clin Cancer Res*. 2018:1–14.

**Ready to submit your research? Choose BMC and benefit from:**

- fast, convenient online submission
- thorough peer review by experienced researchers in your field
- rapid publication on acceptance
- support for research data, including large and complex data types
- gold Open Access which fosters wider collaboration and increased citations
- maximum visibility for your research: over 100M website views per year

**At BMC, research is always in progress.**

Learn more [biomedcentral.com/submissions](https://biomedcentral.com/submissions)

